Scattering of H atoms on a Kr atom

Jacopo Cocomello, Antonio Anna Mele, Luca Zuanazzi

March 2020

One dimensional harmonic oscillator

Consider the dimensionless Hamiltonian of a one dimensional harmonic oscillator

$$H = -\frac{1}{2}\frac{d^2}{dx^2} + \frac{1}{2}x^2 \tag{1}$$

Our aim is to numerically find the bound states and the corresponding energies. We then have to solve the stationary Schrödinger equation

$$H\psi = E\psi \tag{2}$$

To do so we use the Numerov algorithm which solves a generic equation

$$\frac{d^2y}{dx^2}(x) + k^2(x)y(x) = s(x) \tag{3}$$

with the following recursion formula

$$y_{i+1}\left(1 + \frac{h^2}{12}k_{i+1}^2\right) - y_i\left(1 - \frac{5h^2}{6}k_i^2\right) + y_{i-1}\left(1 + \frac{h^2}{12}k_{i-1}^2\right) = s_{i+1} - 2s_i + s_{i-1} + \mathcal{O}\big(h^6\big) \tag{4}$$

where the subscript i means evaluated at x_i, the i-th point of a mesh with spacing h. In our case $s = 0$ and $k^2(x) = 2E - x^2$. Obviously, we can't propagate the solution from $x = -\infty$ to $x = +\infty$, hence we start from a *far* point $x_{-n} = -x_{max}$ and propagate up to $x_n = x_{max}$. The spacing of the mesh is then given by $hn = x_{max}$.
The Numerov algorithm requires two initial conditions, we choose $y_{-n} = 0$ and $y_{-n+1} = h$. The former comes from the fact that we're looking for bound states which at infinity, for us represented by x_{max}, tend to zero. The latter is actually an arbitrary constant which affects only the normalization of the resulting wave function. We could as well have used the well known asymptotic gaussian behaviour of the harmonic oscillator bound states, setting $y_{-n} = e^{-x_{max}^2/2}$ and $y_{-n+1} = e^{-(x_{max}-h)^2/2}$, but actually, if x_{max} is sufficiently large, such knowledge is not needed.
The Numerov algorithm also needs the value of E to calculate the solution but only a discrete set of unknown energies is allowed. By that we mean that only for some specific value of E the solution of the Schrödinger equation is a physical bound state, otherwise the wave function will diverge to plus or minus infinity for $x \to \infty$. What we do then is to look for the value of E that produces $y_n = 0$. Therefore, the whole problem can be rephrased as a root-finding problem, which can be tackled with an algorithm like the one of the secant method. In practice, from a starting value of the energy, we examine small contiguous intervals and apply the secant method to those in which y_n changes sign at the edges. We iterate until we find the desired amount of bound states.
In the following graphs (Figure 1) we present the first five bound states found setting $x_{max} = 7$ and $n = 50000$.

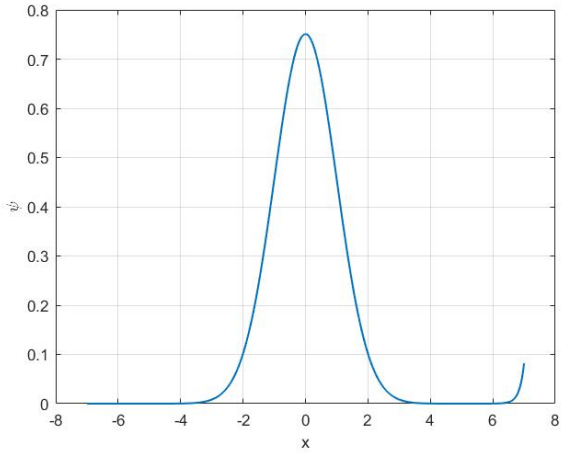

(a) $E_0 = 0.49999999998 \pm 0.00000000001$

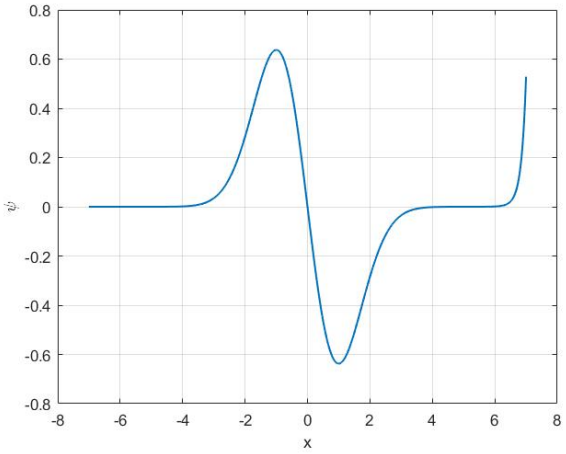

(b) $E_1 = 1.5000000007 \pm 0.0000000006$

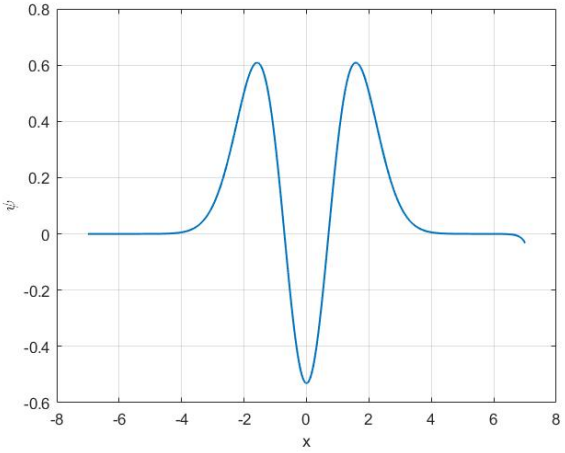

(c) $E_2 = 2.5000000002 \pm 0.0000000003$

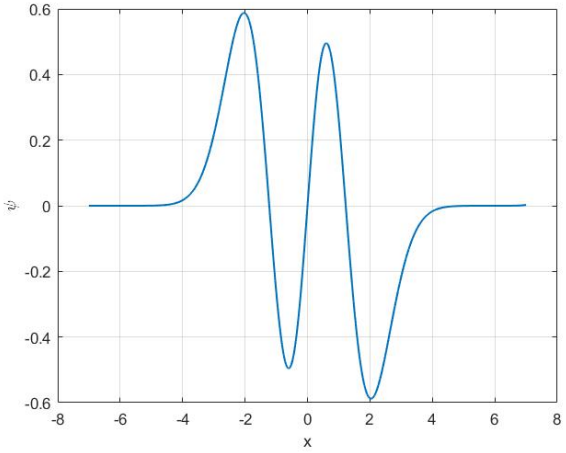

(d) $E_3 = 3.5000000001 \pm 0.0000000001$

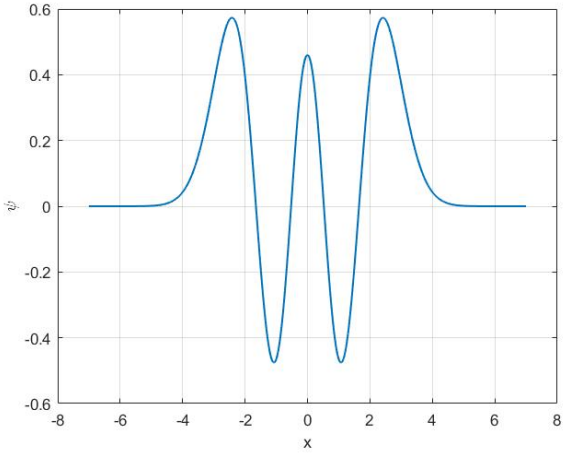

(e) $E_4 = 4.50000000004 \pm 0.00000000004$

Figure 1: Bound states obtained with $x_{max} = 7$ and $n = 50000$.

The errors in the obtained eigenvalues come from the precision limit requested in the secant method. Notice that the wave function close to x_{max} can assume a very unphysical behaviour, like the one of Figure 1b. This is due to the fact that the eigenvalue will never be exact to all the digits, thus at a sufficiently great distance the solution will show instability. This doesn't compromise the correctness of the eigenvalue, which has the value for which such behaviour is mostly restrained.

As a further check on the correctness of the algorithm, it is interesting to see how the eigenvalues vary with respect to the two parameters n and x_{max}.

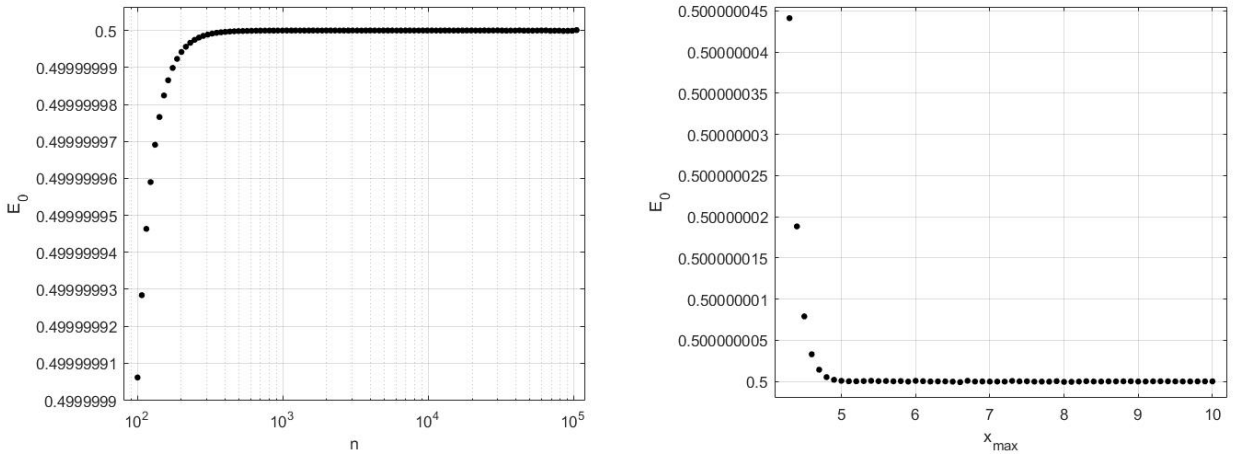

(a) E_0 as function of n with $x_{max} = 7$. **(b)** E_0 as function of x_{max} with $n = 50000$.

Figure 2: Plot of E_0 as function of the two parameters n and x_{max}.

As it could have been expected, the algorithm converges to some eigenvalue as the number of points of the mesh increases. More particularly, one can see from Figure 2a that such convergence is very vast; for $n \gtrsim 100$ the relative error on the energy is already smaller than 10^{-7}. The same amount of error occurs for $x_{max} \gtrsim 4.3$, as one can see from Figure 2b. Remember that the approximation we made $y_{\pm n} = 0$ is more valid as x_{max} increases.

Three dimensional harmonic oscillator

Consider now the dimensionless Hamiltonian of a three dimensional harmonic oscillator

$$H = -\frac{1}{2}\nabla^2 + \frac{1}{2}r^2 \tag{5}$$

Since the potential is spherically symmetric, the solution of the Schrödinger equation can be written as a product of a radial function with a spherical harmonic, namely

$$\psi(\mathbf{r}) = \frac{u_{n,l}(r)}{r} Y_{n,l}(\Omega) \tag{6}$$

We can then focus only on the radial Schrödinger equation

$$\left(-\frac{1}{2}\frac{d^2}{dr^2} + \frac{1}{2}r^2 + \frac{l(l+1)}{2r^2}\right) u_{n,l} = E_{n,l} u_{n,l} \tag{7}$$

which can be solved with the Numerov method, analogously of what done in the one dimensional case. This time $k^2(r) = 2E - r^2 + l(l+1)/r^2$ and we propagate the solution from $r_0 = 0$ up to $r_n = r_{max}$. As initial conditions we set $(u_{n,l})_{i=0} = 0$ and $(u_{n,l})_{i=1} = h^{l+1}$, since we know that any regular solution of the Schrödinger equation must satisfy $\psi(r \to 0) \propto r^l$.
In Figure 3 we plot the solutions for $l = 0, 1, 2$ and for the first three value of the principal quantum number n.

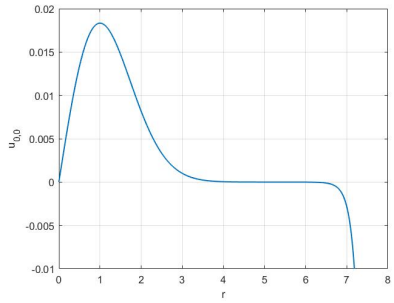

(a) $E_{0,0} = 1.5 + (1 \pm 2)10^{-10}$

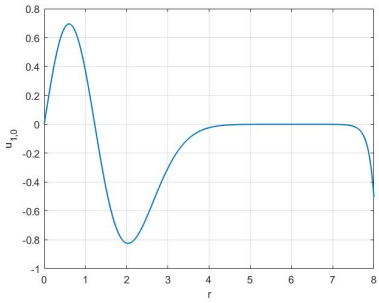

(b) $E_{1,0} = 3.5 + (2 \pm 2)10^{-11}$

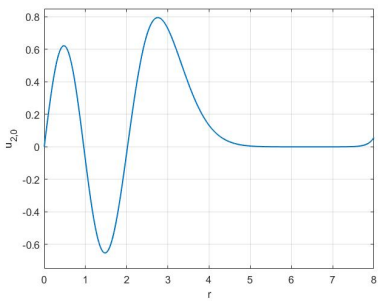

(c) $E_{2,0} = 5.5 + (3 \pm 8)10^{-11}$

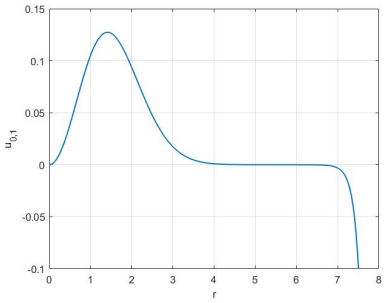

(d) $E_{0,1} = 2.5 + (2 \pm 2)10^{-10}$

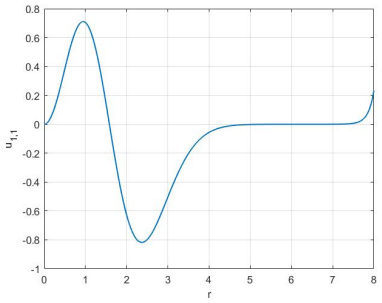

(e) $E_{1,1} = 4.5 + (-4 \pm 7)10^{-11}$

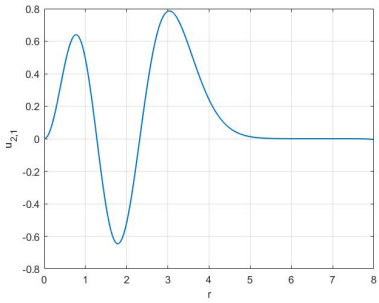

(f) $E_{2,1} = 6.5 + (-1 \pm 4)10^{-11}$

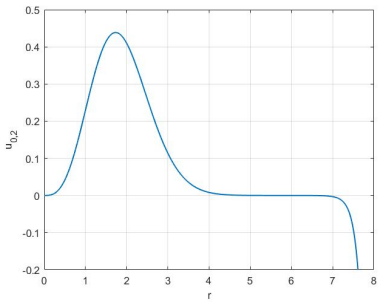

(g) $E_{0,2} = 3.5 + (2 \pm 2)10^{-10}$

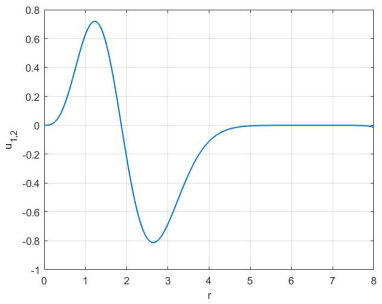

(h) $E_{1,2} = 5.5 + (10 \pm 2)10^{-11}$

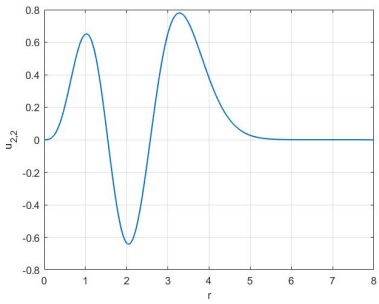

(i) $E_{2,2} = 7.5 + (1 \pm 3)10^{-11}$

Figure 3: Bound states obtained with $r_{max} = 8$ and $n = 100000$.

Bessel functions

An algorithm has been written to obtain spherical Bessel's functions, both regular and irregular ones (Von Neumann's and Bessel's). A simple rule was applied, namely, said $s_l(x)$ a general spherical Bessel function it is true that

$$s_{l+1}(x) = \frac{2l+1}{x} s_l(x) - s_{l-1}(x), \tag{8}$$

with the initial conditions changing for regular or irregular behaviour;

$$j_{-1}(x) = \frac{\cos(x)}{x}, \qquad j_0(x) = \frac{\sin(x)}{x}, \tag{9}$$

for spherical Bessel functions and

$$n_{-1}(x) = \frac{\sin(x)}{x}, \qquad n_0(x) = -\frac{\cos(x)}{x}. \tag{10}$$

for Von Neumann functions. The code is written in a recursive way, such that once one has established which regularity and order are needed the function that calculates $s_l(x)$ is recursively called such to calculate all the smaller order functions which are necessary.

Adimensional radial Schrödinger equation

The aim now is to rescale the radial Schrödinger equation

$$\left(-\frac{\hbar^2}{2m}\frac{d^2}{dr^2}+v(r)+\frac{\hbar^2}{2m}\frac{l(l+1)}{r^2}\right)u_{n,l}=E_{n,l}u_{n,l} \tag{11}$$

with appropriate units dictated by the interaction potential considered, which is

$$v(r)=4\epsilon\left[\left(\frac{\sigma}{r}\right)^{12}-\left(\frac{\sigma}{r}\right)^{6}\right] \tag{12}$$

Using a Lennard-Jones potential it is natural to express energies in unit of ϵ and distances in unit of σ: $r=x\sigma$ and $E_{n,l}=\eta_{n,l}\epsilon$, with x and η adimensional distance and energy. So the Schrödinger equation reads

$$\begin{aligned}
&-\frac{\hbar^2}{2m}\frac{\mathrm{d}^2u_{n,l}}{\mathrm{d}(x\sigma)^2}+4\epsilon\left[\left(\frac{\sigma}{x\sigma}\right)^{12}-\left(\frac{\sigma}{x\sigma}\right)^{6}\right]u_{n,l}+\frac{\hbar^2}{2m}\frac{l(l+1)}{(x\sigma)^2}u_{n,l}=\eta_{n,l}\epsilon u_{n,l}\\
&-\frac{\hbar^2}{2m\sigma^2}\frac{\mathrm{d}^2u_{n,l}}{\mathrm{d}x^2}+4\epsilon\left[\left(\frac{1}{x}\right)^{12}-\left(\frac{1}{x}\right)^{6}\right]u_{n,l}+\frac{\hbar^2}{2m\sigma^2}\frac{l(l+1)}{x^2}u_{n,l}=\eta_{n,l}\epsilon u_{n,l}
\end{aligned} \tag{13}$$

Furthermore, we can divide the whole equation by ϵ and find

$$-\beta\frac{\mathrm{d}^2u_{n,l}}{\mathrm{d}x^2}+4\left(x^{-12}-x^{-6}\right)u_{n,l}+\beta\frac{l(l+1)}{x^2}u_{n,l}=\eta_{n,l}u_{n,l} \tag{14}$$

so that the new form of the radial Schrödinger equation deals with some adimensional distances and energy and all the physical scales of the problem are contained in the multiplicative constant

$$\beta=\frac{\hbar^2}{2m\epsilon\sigma^2} \tag{15}$$

In our case the Lennard-Jones potential models the interaction in a H-Kr elastic scattering process. The specific values of the Lennard-Jones parameters are $\epsilon=5.9\,\mathrm{meV}$ and $\sigma=3.18\,\text{Å}$ and m is the reduced mass of the system, namely $m\simeq 0.9959\,\mathrm{u}$. The constant β then turns out to be approximately

$$\beta\simeq 0.03518 \tag{16}$$

Approximation near the origin

We want to prove that the function

$$u(r)=A\exp\left(-\frac{b^5}{r^5}\right)=A\exp\left(-\frac{b^5}{\sigma^5x^5}\right) \tag{17}$$

is a solution of the radial Schrödinger equation (14) in the limit $r\to 0$.
Firstly, we calculate the second derivative of u:

$$\frac{\mathrm{d}^2u(x)}{\mathrm{d}x^2}=\frac{\mathrm{d}}{\mathrm{d}x}\left[\frac{5b^5}{\sigma^5x^6}u(x)\right]=-\left(\frac{30b^5}{\sigma^5x^7}-\frac{25b^{10}}{\sigma^{10}x^{12}}\right)u(x) \tag{18}$$

Then we have to insert this expression in the radial Schrödinger equation (14)

$$\beta\left(\frac{30b^5}{\sigma^5x^7}-\frac{25b^{10}}{\sigma^{10}x^{12}}\right)u(x)+4\left(x^{-12}-x^{-6}\right)u(x)+\beta\frac{l(l+1)}{x^2}u(x)=\eta u(x) \tag{19}$$

Notice that $u(x)$ is a multiplicative function that can be factorized

$$\left[\beta\left(\frac{30b^5}{\sigma^5 x^7}-\frac{25b^{10}}{\sigma^{10}x^{12}}\right)+4\left(\frac{1}{x^{12}}-\frac{1}{x^6}\right)+\beta\frac{l(l+1)}{x^2}-\eta\right]u(x)=0 \tag{20}$$

Now we consider the limit for $x\to 0$, hence in the square parenthesis we keep only the leading power of x, namely x^{-12}

$$\left(-\beta\frac{25b^{10}}{\sigma^{10}}+4+\mathcal{O}\left(x^5\right)\right)\frac{u(x)}{x^{12}}=0 \tag{21}$$

Such equation is satisfied, for $x\to 0$, if

$$-\beta\frac{25b^{10}}{\sigma^{10}}+4=0 \qquad \Longrightarrow \qquad b=\sigma\left(\frac{4}{25\beta}\right)^{\frac{1}{10}} \tag{22}$$

Therefore we have shown that the function

$$u(x)=A\exp\left(-\frac{2}{5\sqrt{\beta}x^5}\right) \tag{23}$$

is the asymptotic solution to the radial Schrödinger equation (14), in the limit $x\to 0$.

Phase shift

In order to calculate the phase shift δ_l we apply the following formula

$$\delta_l=\arctan\left(\frac{\kappa j_l\left(kr_2\right)-j_l\left(kr_1\right)}{\kappa n_l\left(kr_2\right)-n_l\left(kr_1\right)}\right) \tag{24}$$

where $\kappa=\frac{u_l(r_1)r_2}{u_l(r_2)r_1}$. For k, since in our units $E=\eta\epsilon$, we have:

$$k=\sqrt{\frac{2mE}{\hbar^2}}=\sqrt{\frac{2m\eta\epsilon}{\hbar^2}}=\frac{1}{\sigma}\sqrt{\frac{2m\eta\epsilon\sigma^2}{\hbar^2}}=\frac{1}{\sigma}\sqrt{\frac{\eta}{\beta}} \tag{25}$$

Moreover, we defined $r=\sigma x$, hence

$$kr_i=\sqrt{\frac{\eta}{\beta}}x_i \tag{26}$$

We can compute the terms $j_l\left(kr_i\right)$ and $n_l(kr_i)$ that appear in equation (24) with the method developed in the previous section, see equaton (8).
At this point, we only need to calculate

$$\kappa=\frac{u_l\left(r_1\right)r_2}{u_l\left(r_2\right)r_1}=\frac{u_l\left(\sqrt{\eta/\beta}\,x_1\right)x_2}{u_l\left(\sqrt{\eta/\beta}\,x_2\right)x_1} \tag{27}$$

In order to do that we need to find the solution of equation (17), which can be written as

$$\frac{\mathrm{d}^2u_l}{\mathrm{d}x^2}-\frac{1}{\beta}\left[4\left(x^{-12}-x^{-6}\right)+\beta\frac{l(l+1)}{x^2}-\eta\right]u_l=0 \tag{28}$$

and can be solved with the Numerov method. This time $k^2(r)=\dfrac{1}{\beta}\left[\eta-4\left(x^{-12}-x^{-6}\right)-\beta\frac{l(l+1)}{x^2}\right]$ and we propagate the solution from x_{low} up to $x_n=x_{max}$. Furthermore, we use $n=250000$

and $x_{max} = 15$. For small x we use the asymptotic solution we found in the previous section, namely

$$u_l(x) = \exp\left(-\frac{2}{5\sqrt{\beta}x^5}\right) \qquad \forall\, x \in (0,\, x_{low}) \tag{29}$$

As requested we pick $x_{max} \geq x_2 \geq x_1 > 5$, $0 < x_{low} < 0.5$ and $\eta = 0.3$.
In Figure 4 we present the phase shifts for the first value of the angular momentum quantum number l.

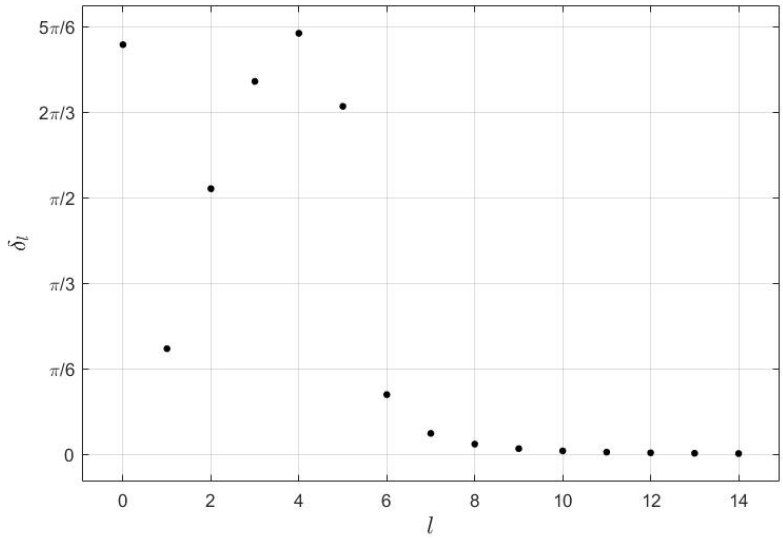

Figure 4: Phase shifts calculated with $x_{low} = 0.4$, $x_1 = 14$ and $x_2 = 14.2$.

Notice that δ_l rapidly goes to zero as l increases, therefore any practical calculation can take into account only the first phase shifts and neglect all the others. Such behaviour can be explained with the following consideration. We can define the effective potential $V_l(x) = 4\,(x^{-12} - x^{-6})\,u_{n,l} + \beta l(l+1)x^{-2}$, which is very close to the actual potential (12) for $r \to 0$ while at great distances the centrifugal part dominates (see Figure 5).

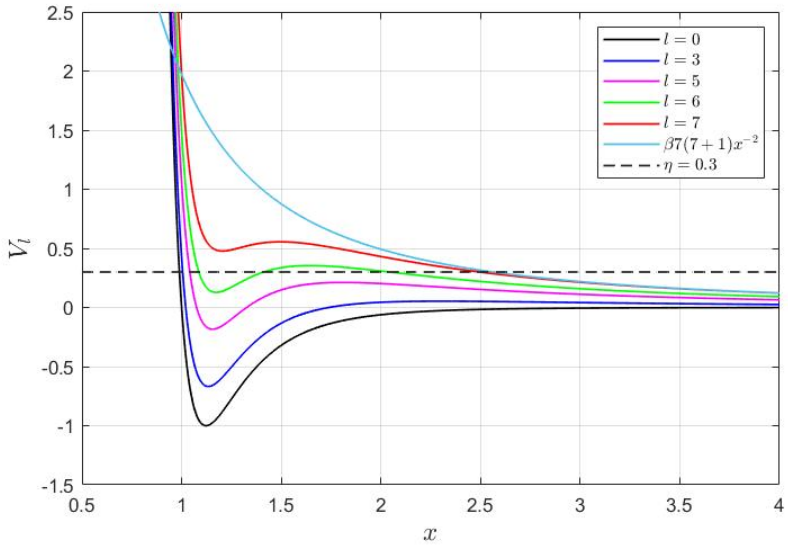

Figure 5: Effective potential V_l for different values of l and centrifugal potential superimposed.

The interesting thing is that we can still see the minimum of the Lennard-Jones potential only for low values of l while, for $l \geq 7$, the part of the potential below the energy as our scattering process η is almost the same of the centrifugal potential. This means that, the potential felt for small values of l is a lot different than the free potential, that is the centrifugal part, hence the real wave function deviates from the free solution with a considerably δ_l. On the contrary, if $l \geq 7$ the potential felt is similar to the free one, hence no considerable deviation appears between the wave functions and δ_l is small. Obviously, increasing the energy η as we will do in the next section, we are probing details of a closer interaction, making more phase shifts become relevant.
To investigate the stability of our results with respect to our parameters we present some graphs showing the variations of the first phase shift δ_0 and the corresponding radial wave function u_0 (Figure 6).

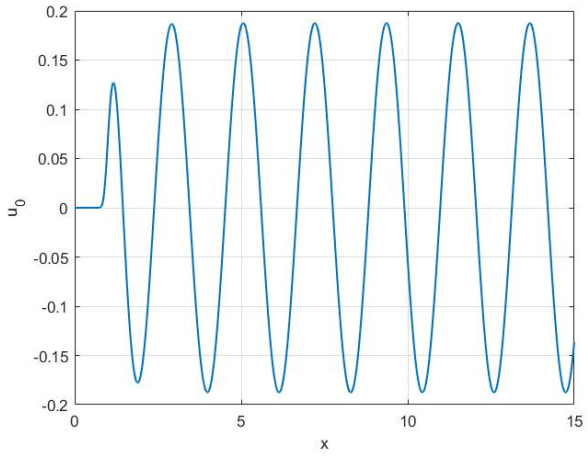

(a) Radial wave function for $x_{low} = 0.4$.

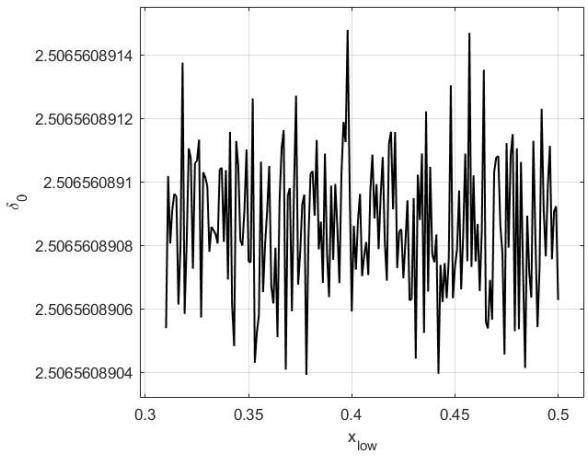

(b) δ_0 with $x_1 = 14$ and $x_2 = 14.2$.

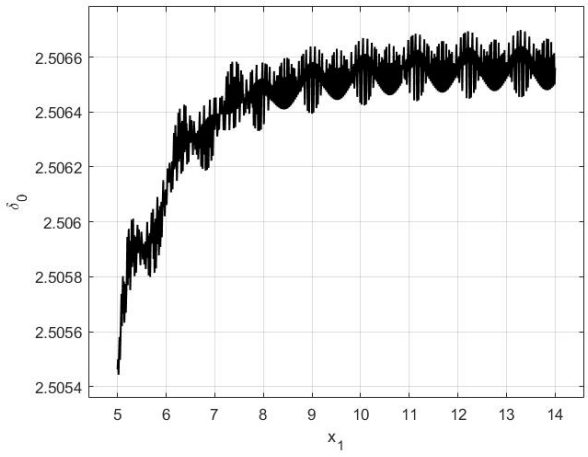

(c) δ_0 with $x_2 = x_1 + 0.2$ and $x_{low} = 0.4$.

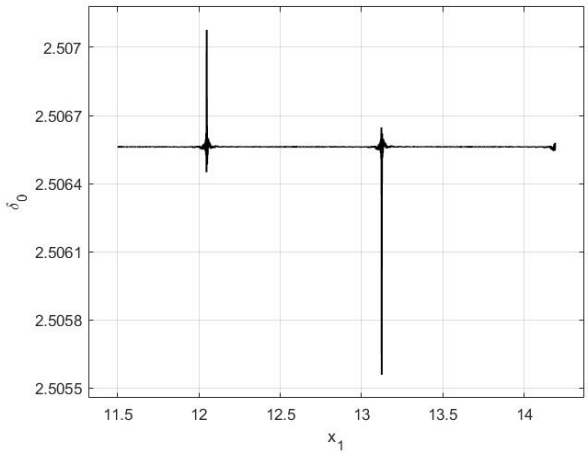

(d) δ_0 with $x_2 = 14.2$ and $x_{low} = 0.4$.

Figure 6: Variations of δ_0 and radial wave function u_0

From Figure 6a we see that the radial wave function, already for $x \gtrsim 5$, assumes the sinusoidal shape characterizing a free solution of the Schrödinger equation. From Figure 6b we see that δ_0 has small, random variations as function of x_{low}, probably due to some numerical error. If instead we vary x_1, keeping the interval $x_2 - x_1$ fixed, we see from Figure 6c that δ_0 converges to some value with not so small numerical noise. The plot is similar if instead of $x_2 - x_1 = 0.2$ we choose any number up to about one. The variation of δ_0 with respect to the distance $x_2 - x_1$ is shown in Figure 6d, where we vary x_1 keeping x_2 fixed. We can see that δ_0 is constant

(modulo small numerical variations) except for some particular periodic values of $x_2 - x_1$. At those points, both numerator and denominator of the arc tangent in equation (24) go to zero, making the division particularly subjected to numerical errors.
The plots for different values of l are analogous of the ones shown for $l = 0$.

Total cross-section

The total cross section $\sigma_{tot}(k)$ has been found through the relation

$$\sigma_{tot}(k) = \frac{4\pi}{k^2} \sum_{l=0}^{\infty} (2l+1) \sin^2(\delta_l(k)) \tag{30}$$

which can be rewritten in units of σ and ϵ as

$$\frac{\sigma_{tot}(\eta)}{\sigma^2} = \frac{4\pi\beta}{\eta} \sum_{l=0}^{6} (2l+1) \sin^2\left(\delta_l(\eta)\right) \tag{31}$$

where we restricted the sum to only the first 7 phase shifts.
To calculate the phase shifts we make use of the algorithm created for previous paragraph and apply it in the energy range $[0,\, 0.59]\epsilon$. In Figure 7 we plot the obtained total cross section. Notice that there are two major peaks which dominate the behaviour of the cross section.

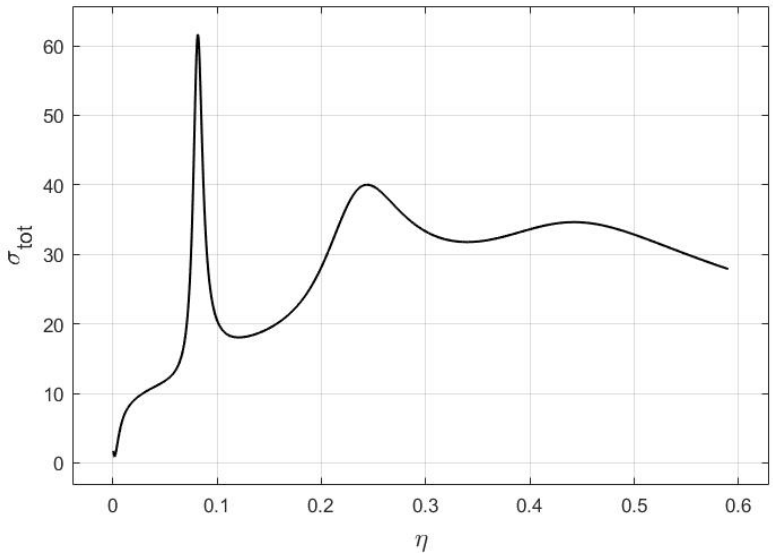

Figure 7: Total cross section as function of energy in unit of σ^2.

The peaks can be explained as resonances of the two body system due to $l = 4$ and $l = 5$ effective interaction. In Figure 8 we show the different partial wave's contributions to the total cross section.

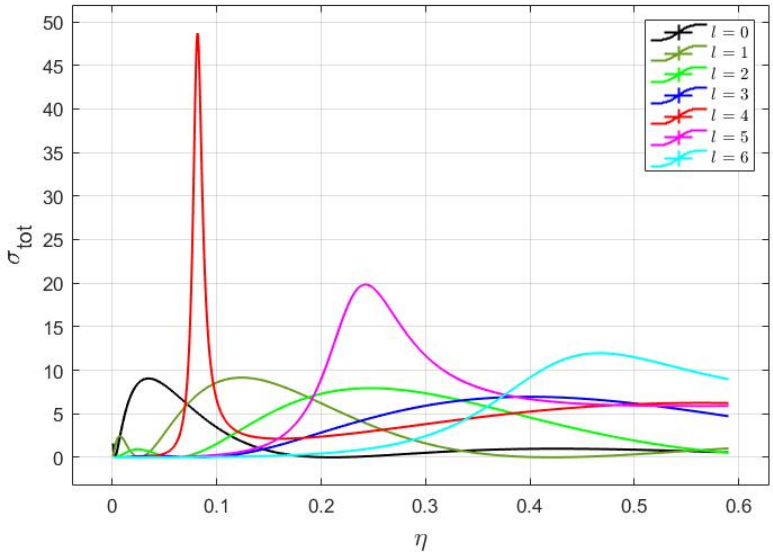

Figure 8: Partial wave's contributions to the total cross section.

One may see that major contributions are given by partial waves with $l = 4, 5, 6$. Contributions for higher angular momentum are negligible in the interested range of energies; this supports our approximation to truncate the infinite sum in equation (30) to $l = 6$. In order to explicitly show the error made neglecting partial waves with $l > 6$, in Figure 9 we compare the previous total cross section with the one calculated truncating the sum to $l = 20$.

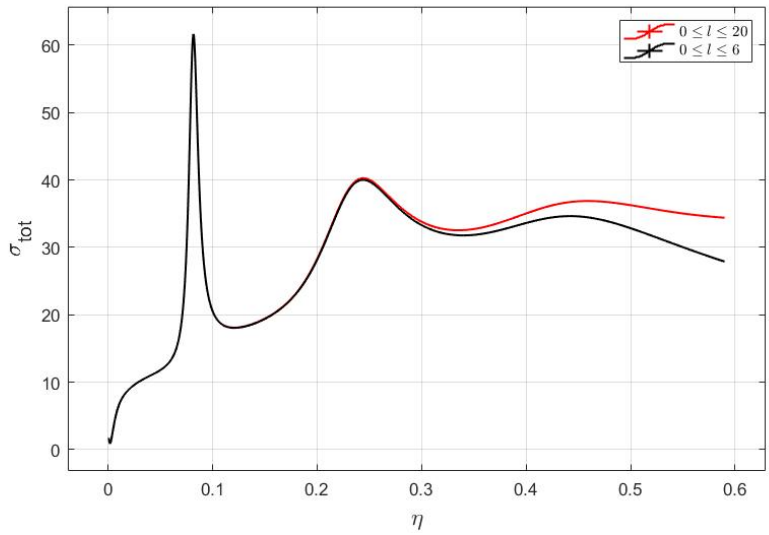

Figure 9: Total cross sections obtained summing partial waves up to $l = 6$ and $l = 20$ superimposed.

It is evident that contributions for $l > 6$ only matter for higher values on energies in the interval $[0, 0.59]\epsilon$ but anyway do not give rise to any other resonance phenomena.
A possible explanation, at least for $l > 7$, is found in the argument presented in the previous paragraph, as for $l > 7$ the effective potential is only intercepted by the atoms relative energy in the hard-core region. For the specific value of $l = 7$ the issue is more subtle: in Figure (9) we see that including higher values of momenta has only the effect to slightly increase the cross section for higher energies in the interval introducing no resonant peak. This may be because the very small well of effective potential for $l = 7$ is not enough to intercept any semi-bound

vibrational state, hence the two body system does not experience any effective binding force that may keep the atoms closer for a finite amount of time.

Our results can be compared with those shown in the reference report by Toennies, Welz and Wolf published on the Journal of Chemical Physics that we were given. They made a similar analysis of phase shifts and cross sections was made for the same system we specialized on, H-Kr. A major difference has to be pointed out, which is the choice of parameters for Lennard-Jones interaction potential: the value of energy potential at its minimum was chosen the same, $\epsilon = 5.90\,\text{meV}$, but hardcore repulsion region is different, for we used $\sigma = 3.18\,\text{Å}$ while in the reference $\sigma = 3.57\,\text{Å}$. This leads to a slightly different value of the constant β and hence to a minor change in the value of cross section at its peaks. To put it more quantitatively

$$\beta_{reference} = \beta \frac{\sigma^2}{\sigma^2_{reference}} = 0.02791 \tag{32}$$

against our $\beta = 0.03518$.
However, this slight change does not affect the position of the peaks, with respect to energy, and therefore neither the value of phase shifts, modulo π, varies significatively.
Measurements of resonances energies are reported in the reference:

C.o.M. energy $[\epsilon]$	l
0.085 ± 0.004	4
0.27 ± 0.01	5
0.5 ± 0.02	6

Table 1: Measured energies for resonances of the H-Kr system in the reference paper.

The differences in energy values may be due neglecting higher momentum corrections for higher values of energy in the range. In fact the energy for the $l = 4$ resonance is the most compatible with our numerical results. Furthermore we can appreciate how the position of $l = 6$ resonance peak slightly increases by considering contributions to the total cross section coming from higher values of momenta, $l \in [0, 20]$. We expect that a calculation which involves much more values of l may get the resonance peak even nearer to the measured value of resonance energy.